PLOS ONE

RESEARCH ARTICLE

RNA Sequencing Reveals a Slow to Fast Muscle Fiber Type Transition after Olanzapine Infusion in Rats

Christopher J. Lynch[1]*, Yuping Xu[1], Andras Hajnal[2], Anna C. Salzberg[3], Yuka Imamura Kawasawa[4,5,6]

1 Department of Cellular and Molecular Physiology, College of Medicine, Penn State University, Hershey, Pennsylvania, 17033, United States of America, **2** Department of Neural and Behavioral Sciences, College of Medicine, Penn State University, Hershey, Pennsylvania, 17033, United States of America, **3** Department of Public Health Sciences, College of Medicine, Penn State University, Hershey, Pennsylvania, 17033, United States of America, **4** Department of Pharmacology, College of Medicine, Penn State University, Hershey, Pennsylvania, 17033, United States of America, **5** Department of Biochemistry and Molecular Biology, College of Medicine, Penn State University, Hershey, Pennsylvania, 17033, United States of America, **6** The Institute for Personalized Medicine, College of Medicine, Penn State University, Hershey, Pennsylvania, 17033, United States of America

* clynch@hmc.psu.edu

OPEN ACCESS

Citation: Lynch CJ, Xu Y, Hajnal A, Salzberg AC, Kawasawa YI (2015) RNA Sequencing Reveals a Slow to Fast Muscle Fiber Type Transition after Olanzapine Infusion in Rats. PLoS ONE 10(4): e0123966. doi:10.1371/journal.pone.0123966

Academic Editor: Guillermo López Lluch, Universidad Pablo de Olavide, Centro Andaluz de Biología del Desarrollo-CSIC, SPAIN

Received: December 15, 2014

Accepted: March 2, 2015

Published: April 20, 2015

Data Availability Statement: Data are available within the paper, are included as Supporting Information, and the Illumina fastq file have been deposited with the National Center for Biotechnology Information (NCBI) Gene Expression Omnibus database (GEO Accession number: GSE65787).

Funding: The study was funded by National Institute of Diabetes and Digestive and Kidney Diseases (NIDDK: http://www.niddk.nih.gov/Pages/default.aspx) grant DK084428. The funders had no role in study design, data collection and analysis, decision to publish, or preparation of the manuscript.

Abstract

Second generation antipsychotics (SGAs), like olanzapine, exhibit acute metabolic side effects leading to metabolic inflexibility, hyperglycemia, adiposity and diabetes. Understanding how SGAs affect the skeletal muscle transcriptome could elucidate approaches for mitigating these side effects. Male Sprague-Dawley rats were infused intravenously with vehicle or olanzapine for 24h using a dose leading to a mild hyperglycemia. RNA-Seq was performed on gastrocnemius muscle, followed by alignment of the data with the Rat Genome Assembly 5.0. Olanzapine altered expression of 1347 out of 26407 genes. Genes encoding skeletal muscle fiber-type specific sarcomeric, ion channel, glycolytic, O_2- and Ca^{2+}-handling, TCA cycle, vascularization and lipid oxidation proteins and pathways, along with NADH shuttles and LDH isoforms were affected. Bioinformatics analyses indicate that olanzapine decreased the expression of slower and more oxidative fiber type genes (e.g., type 1), while up regulating those for the most glycolytic and least metabolically flexible, fast twitch fiber type, IIb. Protein turnover genes, necessary to bring about transition, were also up regulated. Potential upstream regulators were also identified. Olanzapine appears to be rapidly affecting the muscle transcriptome to bring about a change to a fast-glycolytic fiber type. Such fiber types are more susceptible than slow muscle to atrophy, and such transitions are observed in chronic metabolic diseases. Thus these effects could contribute to the altered body composition and metabolic disease olanzapine causes. A potential interventional strategy is implicated because aerobic exercise, in contrast to resistance exercise, can oppose such slow to fast fiber transitions.

Competing Interests: The authors have declared that no competing interests exist.

Introduction

Second generation antipsychotics (SGAs, also called, atypical antipsychotics), like olanzapine, are used to treat schizophrenia and bipolar disorder [1]. Owing to superior efficacy for psychiatric disorders compared to first generation drugs and a growing number of off- and on-label indications, the rate of new antipsychotic prescriptions has been growing steadily for adults and children [2]. For example, 2011 estimates indicated 3.1 million Americans were prescribed antipsychotics, up 13% from the year before [3]. Unfortunately, some SGAs cause adverse metabolic side effects that can negatively impact patient compliance. These side effects include hyperglycemia, glucose intolerance, weight gain, dyslipidemia, obesity, hyperglycemia, type 2 diabetes (T2D), ketoacidosis and even death [4–10]. Olanzapine and clozapine are two examples that may cause average body weight gains in the range to 1 pound per week [11].

While weight gain contributes to the metabolic complications of SGAs, there is strong evidence of body weight independent metabolic effects preceding obesity and type 2 diabetes. For example, dyslipidemia, hyperglycemia and glucose intolerance can be observed minutes or days after SGA administration, associated with rapid changes in muscle metabolism [12]. Endocrine-metabolic effects observed in plasma are sustained for weeks in healthy subjects and high fidelity preclinical models, prior to alterations in body composition/weight gain and increased hunger that appear later [11, 13–16]. Therefore understanding acute actions of SGAs might elucidate mechanisms contributing to these side effects.

Skeletal muscle is one of the most important tissues by weight for the disposal of glucose and macronutrients. As a major component of whole body energy balance it has the potential to impact the acute effects of SGAs on glycemia and glucose tolerance. Chronic olanzapine treatment in rats and dogs increased adiposity but not body weight [17–19]. This implies that changes in lean mass could be occurring, conceivably altering muscle energy requirements, susceptibility to atrophy and glycemia. Such changes could facilitate the adiposity elicited by olanzapine [17–19]. More information on how SGAs affects skeletal muscle is needed.

Skeletal muscles exhibit different fiber types with distinct features and energy requirements. While various classification schemes a simple classification is slow (oxidative, SO), intermediate (fast oxidative-glycolytic, FOG) and fast twitch (glycolytic, FG). SO fibers are also called type I, while the fastest-twitch glycolytic fibers (FG) in rats are type IIb. SO fibers contract or twitch more slowly than other types, are more efficient using oxygen to sustain contractions owing to their higher concentration of myoglobin (contributing to darker color), mitochondria and increased vascularity [20, 21]. They express myosin heavy chain 7 (*MYH7*, as found in soleus). At other end of the spectrum, FG fibers (IIb containing *MYH4*) have a very fast twitch force and very high power, but a low capillary density and mitochondrial and myoglobin content reflected in their whiter color [20–22]. Consequently, IIB fibers are less able to oxidize glucose or FFA, and instead, generate more ATP from anaerobic glycolysis. FOG fiber types exhibit intermediate characteristics and unique myosin heavy chains (e.g., *MYH2* and *MYH1*) and can be further sub-divided. An important difference between slower and faster fibers, in addition to energy consumption and twitch speed, is that FG fibers are more susceptible than SO to atrophy arising from various metabolic pathologies [23]. In obesity and T2D, skeletal muscle has been associated with either a loss of oxidative enzyme capacity irrespective of muscle fiber type [24], or a transition of muscle fiber types from more SO to the less metabolically flexible FG fibers [25–29].

Given the importance of skeletal muscle as a major consumer of whole body energy and macronutrients, it is important to understand how olanzapine affects this tissue before significant changes in adiposity occur. Therefore in this study we used RNA-Seq to quantify gene expression in response to continuous infusion of olanzapine for 24h using a protocol that produces a mild hyperglycemia.

Materials and Methods

Ethics Statement

All of the vertebrate animal procedures were approved by the Institutional Animal Care and Use Committee (IACUC) of Penn State University College of Medicine (Hershey, PA). The Animal Resource Program is accredited by AAALAC International. All animal living conditions are consistent with standards laid forth in the Guide for the Care and Use of Laboratory Animals (2011), 8th edition, published by the National Research Council.

Olanzapine infusion

Male Sprague Dawley rats (150–175g) from Charles River Laboratories (Cambridge, MA, USA) were acclimated to single housing for several weeks while being maintained on a 12:12 h light dark cycle at ~21°C and provided free access to water and a standard rodent chow (2018, Harlan Laboratories, Madison, WI). Under brief isoflurane anesthesia, venous (jugular) and arterial (carotid) catheters were surgically implanted as previously described [12, 18] and an external neck collar was placed for use in the CMA/120 infusion system (CMA7431059, Harvard Apparatus, Hollison, MA). A week or more after this surgery, all the experimental animals had regained their body weight trajectories. The night before infusions, rats were individually housed in a CMA/120 Rat System for Freely Moving Animals. They continued to have free access to the same food, water and dried corncob bedding used in the home cages. The next day catheters were connected to the catheter swivel system. Heparinized glucose determinations were obtained as described [12, 18], prior to the start of the infusions study ~2PM. For the olanzapine group, the venous catheter was attached to a New Era Pump Systems syringe pump (Model NE-300) filled with olanzapine (Dr. Reddy's Laboratories Ltd, Hyderabad, India) in sterile saline (infusion: 1mg/100g BW loading dose for 0.5h and then 0.04mg/100g/h continuously for 23.5h). Control rats were infused with vehicle at the same rate and volume. At the conclusion of the infusions additional heparinized plasma and blood glucose determinations were obtained for blood glucose determination. Gastrocnemius was then surgically removed under isoflurane anesthesia (carried with 100% O_2), and frozen between two aluminum blocks cooled to the temperature of liquid nitrogen and then stored at -80°C until RNA was isolated. While under continuous anesthesia, the animals were euthanized by cutting the diaphragm and removing the heart.

RNA Sequencing

Total RNA was extracted as previously described with slight modification [30]. Briefly, frozen muscle tissue was pulverized in liquid nitrogen using mortar and pestle, followed by bead mill homogenization (Bullet Blender, Next Advance) using stainless steel beads (Next Advance, cat# SSB14B) and mirVana RNA isolation kit (Life Technologies). Optical density values of extracted RNA were measured using NanoDrop (Thermo Scientific) to confirm an A_{260}:A_{280} ratio above 1.9. RIN was determined for each sample using Bioanalyzer RNA 6000 Nano Kit (Agilent Technologies). The cDNA libraries were prepared using the TruSeq RNA Sample Prep Kit v2 (Illumina) as per the manufacturer's instructions. The final product was assessed for its size distribution using Bioanalyzer DNA High Sensitivity Kit (Agilent Technologies) and for its concentration using Kapa library quantification kit (Kapa Biosystems). Six libraries were pooled per HiSeq lane, followed by on-board cluster generation on a Rapid Run single-end flow cell and subsequent 50 cycles sequencing (v3 sequencing kit) according to the manufacturer's instructions (HiSeq 2500, Illumina). Demultiplexed and quality filtered mRNA-seq reads were then aligned to Rat reference assembly (Rn5) using TopHat (v.2.0.9). The uniquely

mapped reads were used to calculate the normalized expression level of genes, as fragments per kilobase of exon per million fragments mapped (FPKM), using Cufflinks (v.2.2.1).

Quantitative Real-Time-PCR (QT-RTPCR)

Equal quantities of total RNA were used to synthesize cDNA using the High Capacity cDNA RT Kit with RNase Inhibitors (Applied Biosystems, Inc.). For QRT-PCR reactions, the TaqMan Gene Expression Assays (Applied Biosystems, Inc.) specific for rat *Eef2*, *OSTN*, *Casq2*, *LPL*, *Alp2a2*, *Tnni1*, *Pavlb*, and *TPM1* was performed according to the manufacturer's instructions and was carried out with equal quantities of cDNA. The assays were run on a 7900HT PCR system (Applied Biosystems, Inc.) available at the College of Medicine Core Lab and were analyzed using the comparative Ct method. The results were normalized to internal *Eef2* mRNA controls.

Biostatistics and Bioinformatic Analysis

To determine significant differences in mean FPKM values between control and olanzapine groups, the DEGexp function of the DEGseq 1.18.0 R package was used with the Likelihood Ratio Test (LRT) and default parameters. A $p<0.05$ was used to determine significant differences, however genes where no detectable RNA was observed in some subjects were flagged (#VALUE!) and not considered further. Graphpad Prism 6.0 was used to examine statistical changes in QT-RTPCR data by Students t-test ($p<0.05$ was considered statistically significant) and linear regression analysis.

Functional annotation clustering, pathway analysis and gene ontology along with associated confidences indicating the strength of evidence for pathway effects were obtained using a series of tools including Ingenuity Pathway Analysis (IPA, Ingenuity Systems, www.ingenuity.com). Database for Annotation, Visualization and Integrated Discovery (DAVID, http://david.abcc.ncifcrf.gov/), Kyoto Encyclopedia of Genes and Genomes (KEGG, www.kegg.jp), GeneCards (www.genecards.org) and the Rat Genome Database (RGD, http://rgd.mcw.edu/). Pathway analysis was performed on genes that were statistically different based on DEGSeq analysis. Olanzapine rapidly elevates plasma glucocorticoids as it does glucose [31]. The potential impact of glucocorticoid changes on gene expression and needs to be considered in interpreting the findings [31]. Genes affected by this increase in corticosteroid concentrations were either identified from the above pathway analysis packages or by examining microarray time course data from muscle tissue during constant infusion of methylprednisolone in adrenalectomized rats (NCBI Geo profile GDS2688) [32].

Data Sharing

The processed data (S1 Table), associated metadata, and the "raw" Illumina fastq file have been deposited with the National Center for Biotechnology Information (NCBI) Gene Expression Omnibus database (GEO Accession number: GSE65787).

Results and Discussion

Rats with comparable body weights (vehicle: 373±9g, olanzapine: 388±11g, $p = 0.34$) were infused with vehicle (control) or olanzapine for 24h. The olanzapine infusion produced a modest 30% increase in blood glucose (vehicle, 98±2mg/dl; olanzapine 127±4mg/dl, $p = 0.0023$). This acute effect is consistent with previous findings in humans and animal models, however far greater rises in blood glucose can be achieved with higher doses [31]. Transcriptome sequencing of mRNA of gastrocnemius muscle from rats in the control group resulted in FPKM values expected for striated skeletal muscle tissue. For example, the top one hundred FPKM values

were associated with genes that encode proteins of the skeletal muscle contractile machinery, cation transporters, glycolysis, oxidative metabolism and protein synthesis (S1 Table).

Cluster analysis indicated that the data from each rat clustered into their respective control or OLZ treatment groups (not shown). Of 26,406 genes in the rat genome build we used, 1451 genes were determined to be significantly different due to olanzapine (S1 Table and S2 Table). However 104 of the $p<0.05$ genes were not studied further because the data from DEGexp were flagged ("#Value!", S2 Table) due to no detectable counts in one or more animal (S1 Table).

We next sought to compare genes with statistically different changes due to OLZ according to DEG-Seq to QT-RTPCR data. Our goal was to examine compare these two over different FKPM bin ranges (e.g., with one value below 10,10–100, 100–1000, 1000–10,000 and >10,000) compared to a QT-RTPCR (Fig 1). We endeavored to have at least one OLZ and one Control value in different bins so that more bins could be evaluated. *Ostn*, *Pvalb and Tpm1* expression was significantly elevated by olanzapine treatment based on RNA-Seq and exhibited close proportionally elevated changes based on QT-RTPCR assays using *Eef2* expression as a normalizer. Consistently, olanzapine similarly decreased the expression of *Tnni1*, *Casq2*, *Lpl* and *Atpa2* as determined by either RNA-Seq or QT-RTPCR. The effects of olanzapine based on these two methods were highly correlated (r2 = 0.98, S1 Fig). Thus, these findings suggested that our RNA-Seq data were similarly quantitative as QT-RTPCR, albeit the QT-RTPCR data generally exhibited comparatively higher normalized standard deviations (not shown) as reflected in the size of the standard errors (Fig 1). A weakness is that we did not study QT-RTPCR of genes with lower % FKPM changes, however our conclusions in the results below about affected pathways are largely based on changes in many rather than individual genes. Furthermore, other studies have demonstrated that RNA-Seq is highly accurate for quantifying expression levels [33].

Olanzapine alters skeletal muscle fiber type genes

Bioinformatic analysis of the RNA-Seq data indicates that olanzapine is causing a muscle fiber type transition to the most glycolytic and fastest twitch fiber type (IIb). Multiple lines of evidence support this. The first is an observed decrease in the genes for a number of myosin heavy chain genes and an increase in myosin heavy chain 4, *Myh4* (Table 1). The second is altered expression of other genes and isoforms that comprise fiber type specific components of the muscle sarcomere and muscle cation transporters (Table 1). The categorization of these genes as slow or fast is based on literature along with annotation from the RGD and Genecard databases. Based on these sources, FG fibers (e.g., IIb) normally express higher levels of Actin 3 (*Actn3*), Na^+/K^+-ATPase subunit isoform 2B (*Atp1b2)*, Serca1 (ATPase, Ca^{2+} transporting, cardiac muscle, fast twitch 1;a.k.a., *Atp1a1*), calsequestrin 1 (fast-twitch, skeletal muscle; *Casq1*), myosin, light chain 1, alkali; skeletal, fast (*Myl1*), myosin light chain, (phosphorylatable, fast skeletal muscle; *Mylpf*), myosin binding protein C, fast type (Mybpc2), myomesin 2 (a.k.a. M-protein; *Myom2*), myozenin 1 (a.k.a. calsarcin 2; *Myoz1*), parvalbumin (*Pvalb*), troponin C type 2 (fast;*Tnnc2*), fast skeletal muscle troponin I (*Tnni2*), fast skeletal muscle troponin T gene (*Tnnt3*) and fast twitch tropomyosin 1 (*Tpm1*) [34–48].

In contradistinction to FG fibers, SO fibers express more Actin 2 (*Actn2*), *Atp1a1*, *Atp1b1* (isoforms of Na^+/K^+-ATPase subunits), *Atp2a2 (also called Serca2*: ATPase, Ca^{++} Transporting, Cardiac Muscle, Slow Twitch 2), calsequestrin 2 (*Casq2*), Four-And-A-Half LIM Domains 1 (a.k.a. SLIM1, *Fhl1*), myoglobin (*MB*), myosin binding protein C, slow type (*Mybpc1*), myosin, light chain 2, regulatory, cardiac, slow (*Myl2*), myosin, light chain 3, alkali; ventricular, skeletal, slow (*Myl3*), myomesin 3 (*Myom3*), myogenin (*Myog*), myozenin 2 (a.k.a. calsarcin-1, *Myoz2*), obscurin (*Obscn*), troponin C type 1, slow (*Tnnc1*), troponin I type 1, skeletal, slow (*Tnni1*), tropomyosin 2 beta (*TPM2*) and tropomyosin 3 (*Tpm3*) genes [35, 40,

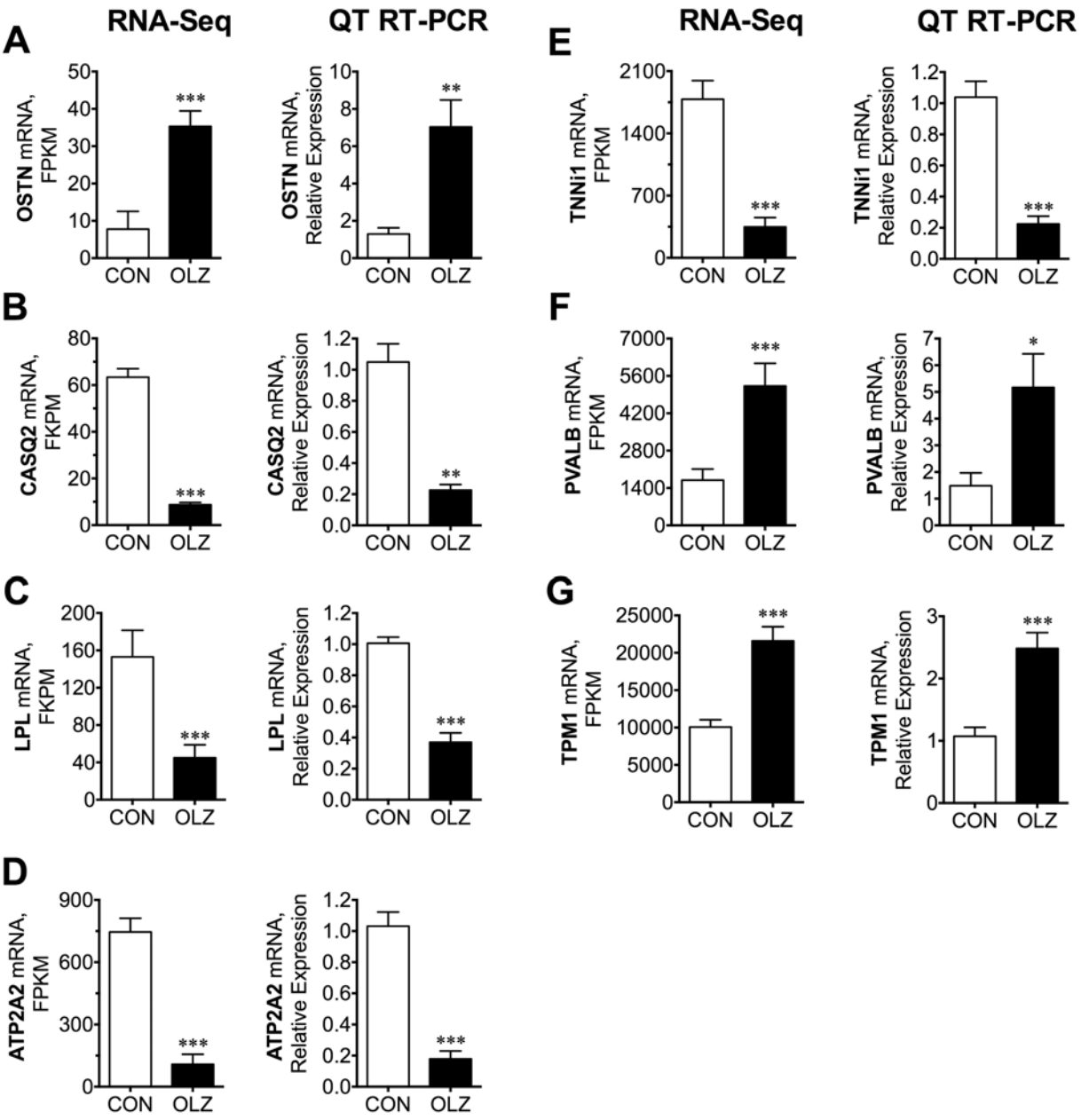

Fig 1. Comparison of RNA-Seq to QT-RTPCR for selected gastrocnemius muscle genes affected by olanzapine infusion. Genes significantly affected by olanzapine infusion based on RNA-Seq were selected for QT-RTPCR analysis using TaqMan gene expression assays using the same preparation of RNA. Genes were selected so that different FKPM size bins (1–10: *OSTN*; 10–99: *OSTN*, *Casq2*, *Lpl*; 100–999: *Lpl*, *Atp2a2*, *Tnni1*, 1000–9000: Tnni, Pvalb; >9000: Tpm1) were represented. The bars show mean± SE. Statistical significance was determined using the DEGSeq R package, which takes into consideration the variability of all of the genes analyzed. QT-RTPCR differences were analyzed using Student's t-test. Asterisk symbols indicate a significant difference compared to control, *: p <0.05, **: p<0.01, ***: p<0.001)

doi:10.1371/journal.pone.0123966.g001

42, 46, 47, 50–54]. Thus, olanzapine infusion reduced the expression of genes encoding contractile and cation transport isoforms found in slow or less glycolytic fast fibers (type 1 & non-IIb, a.k.a., SO & FOG) and up regulated those coding for the most glycolytic type of the fast fibers, type IIb (Table 1). Notably, two of the affected Na^+/K^+-ATPase subunits along with the calcium ATPase, Serca2, have been designated as obesity or T2D candidate genes

Table 1. Olanzapine shifts expression of genes associated with skeletal muscle fiber type.

Fast twitch/ type IIb genes				Slow twitch or intermediate fiber type genes			
Gene name	**Vehicle, FPKM**	**Olanzapine, FPKM**	**Normalized fold change**	**Gene Name**	**Vehicle, FPKM**	**Olanzapine, FPKM**	**Normalized fold change**
Actn3	2145±503	3194±379	+1.4	*Actn2*	1259±5	451±60	-2.9
Atp1b2 *	105±26	162±4.3	+1.5	*Atp1b1* * *Atp1a1*	104±21 34 ±1.3	32±6 23±4.0	-3.4 -1.5
Atp2a1	7138±811	8284±766	+1.2	*Atp2a2* *	793±71	115±48	-7.1
Casq1	1307±218	2295±307	+1.8	*Casq2*	65±4.5	9.2±1.1	-7.3
				Csrp3	419±87	84±16	-5.2
Fhl3	167±31	328±63	+2.0	*Fhl1*	1913±20	491±98	-4.0
				Mb	11791±2736	7193±1471	-1.7
Mybpc2	844±113	1208±149	+1.4	*Mybpc1*	1024±63	469±47	-2.3
Mybph	114±41	229±71	+1.9				
Myh4 (type IIb)	1644±612	2998±373	+1.8	*Myh1* (IIx)	1245±117	787±52	-1.6
				Myh2 (IIa)	361±57	790±24	-4.2
				Myh3	8.8±2.2	2.2±0.7	-8.6
				Myh6	11±2.4	2.7±0.2	-4.3
				Myh7 (I)	653±59	88±44	-7.7
				Myh7b	4.4±0.6	0.66±0.28	-6.9
				Myh8	9.9±2.3	5.3±0.3	-1.9
				Myh10 *	9.2±0.7	1.4±0.2	-6.6
Myl1	12213±951	19839±1339	+1.6	*Myl2*	12267±2974	2364±583	-5.4
Mylpf	15708±1019	38303±5017	+2.4	*Myl3*	3398±602	708±153	-5.0
				Myl6b	312±43	65±32	-5.0
				Myl12a	389±55	215±22	-1.9
Myom2	270±46	256±32	N.S.	*Myom3*	42±3.4	7.1±4.0	-7.2
				Myom1	144±9	114±10	-1.3
				Myog	25±2	12±0.6	-2.3
Myoz1	1354±187	2426±345	+1.8	*Myoz2*	571±83	115±42	-5.1
Pvalb	1778±450	5568±958	+3.0				
				Obscn	93±18	71±6	-1.4
Tnnc2	8963±518	14528±1422	+1.6	*Tnnc1*	2129±331	486±176	-4.6
Tnni2	9604±504	17974±2203	+1.8	*Tnni1*	1595±181	313±93	-5.3
Tnnt3	12592±882	18845±2840	+1.5	*Tnnt1*	2020±380	309±121	-6.8
Tpm1	7939±828	16186±1342	+2.0	*Tpm2*	5455±74	3561±74	-1.6
				Tpm3	1218±186	215±81	-5.9

Isoforms of fast and slow twitch muscle fiber genes with statistically significant changes when comparing Vehicle and Olanzapine groups are indicated by the presence of a normalized fold change value. Data are means plus or minus (±) SE of the fragments per kilobase of exon per million fragments mapped values (FKPM). N.S. indicates no significant difference. An asterisk(*) indicates a prioritized T2D or obesity candidate gene [49].

doi:10.1371/journal.pone.0123966.t001

[49]. Olanzapine also decreased the expression of the gene coding for Muscle LIM protein (*CRP3*, *Csrp3*) which is involved in slow myosin heavy chain expression and fast to slow fiber transitions [55]. While adult rat gastrocnemius is generally considered a mixed muscle, its fiber composition already contains a majority of FG fibers [56]. That explains why the magnitude of the change in IIb-related genes was generally less than the magnitude of lowering of slower twitch fiber associated genes.

Metabolic gene expression in skeletal muscle after olanzapine

Pathway analyses revealed significant changes in glycolysis (p = 1.3E-7), the citrate cycle (TCA cycle, p = 7.7e-14), fatty acid metabolic processes (p = 6.4e-7), and oxidative phosphorylation (p = 1.8e-38) including fatty acid and branched chain amino acid oxidation (p = 1.8e-7). Consistent with a slower to faster fiber type transition, olanzapine increased the expression of most genes in glycolysis (Fig 2A, S3 Table). However, a rate-controlling step in glycolysis, catalyzed by the skeletal muscle isoform of hexokinase (*HK2*), decreased -1.9 fold (Fig 2A, S3 Table). This may be related to the observation that muscle hexokinase, *HK2*, is expressed at higher levels in slower compared to more glycolytic fibers, e.g.: [57]. Notably, muscle hexokinase activity is also depressed in insulin resistance and diabetes [58, 59]. Therefore changes in HK2 are also consistent with the concept of a slow to fast twitch fiber type transition and olanzapine's effect on (Fig 3). FG fibers are more likely to convert pyruvate from glycolysis to lactate and export the lactate rather than oxidizing the pyruvate in mitochondria. Thus consistent with a fiber type transition being underway, olanzapine increased the expression of *Ldha* and *Slc16a3* normally involved in non-oxidative glucose metabolism and cellular lactate efflux, and decreased expression of the genes coding isoforms of lactate dehydrogenase and lactate transporter that have been associated with increased lactate influx and metabolism, *Ldhb and Slc16a1* (also called *MCT1*, see Fig 2A) [60]. Creatine kinase gene expression (*CKM*) was also increased by olanzapine (S1 Table and S2 Table), this too is associated with fiber type switching and anaerobic ATP formation in T2D [61].

In contradistinction to the up-regulation of glycolysis, but consistent with an SO/FOG to FG transition, olanzapine depressed the expression of most TCA cycle genes (Fig 2B and S3 Table). An exception was with isocitrate dehydrogenase (IDH) subunit genes. *Idh3b*, *Idh3a* and *Idh3g* showed inconsistent changes or no significant difference, whereas *Idh3b*, an obesity candidate gene [49], was decreased, as was another IDH (*Idh2*, -2.3 fold) that is highly expressed in gastrocnemius (Fig 2B, S3 Table). However of the genes associated with the pyruvate dehydrogenase complex's entry point into the TCA cycle, only Pdhb and Dld were decreased (S1 Table and S2 Table).

Olanzapine shifted expression of the mitochondrial NAD^+/NADH shuttles used to regenerate NAD^+ for glycolysis (Fig 2C, S1 Table). Genes for the malate aspartate shuttle were decreased, whereas those for the glycerol phosphate shuttle were increased. The observed decrease in malate-aspartate shuttle is consistent with a the concept of a transition being underway to a less oxidative muscle fiber type [62].

Further consistent with a shift to a more glycolytic fiber type, sarcolemmal, cytosolic and mitochondrial genes coding for enzymes and transporters in lipid oxidation were reduced by olanzapine (Table 2). For example, *Lpl* that encodes lipoprotein lipase was -3.5 fold lower. Similarly, gene expression of the sarcolemmal fat transporters, FAT (*Slc27a1*) and fatty acid translocase (*Cd36)* were reduced along with the cytosolic muscle fatty acid binding protein (Fabp3) and enzymes that convert fatty acids to their respective acyl-CoAs were reduced, along with genes for fatty acyl-CoA mitochondrial transport and oxidation, including the rate-controlling step in muscle fatty acid oxidation (*Cpt1b*, Table 2). In contradistinction, olanzapine infusion increased the expression the mitochondrial fatty acid transporter gene, *UCP3*, and that of the adipose tissue specific fatty acid binding protein 4 (*FABP4*, also called *AP2*, Table 2 and S1 Table). While we have no explanation for these changes, it is noted that increased skeletal muscle *UCP3* expression occurs in T2D and during slow to fast twitch muscle fiber type transitions [63, 64]. Furthermore, *FABP4* is the adipose/macrophage fatty acid binding protein, not the muscle specific fatty acid binding protein, FABP3, which did decline (Table 2 and S1 Table). The rise in FABP4 could potentially harken an increase in macrophage presence/inflammation

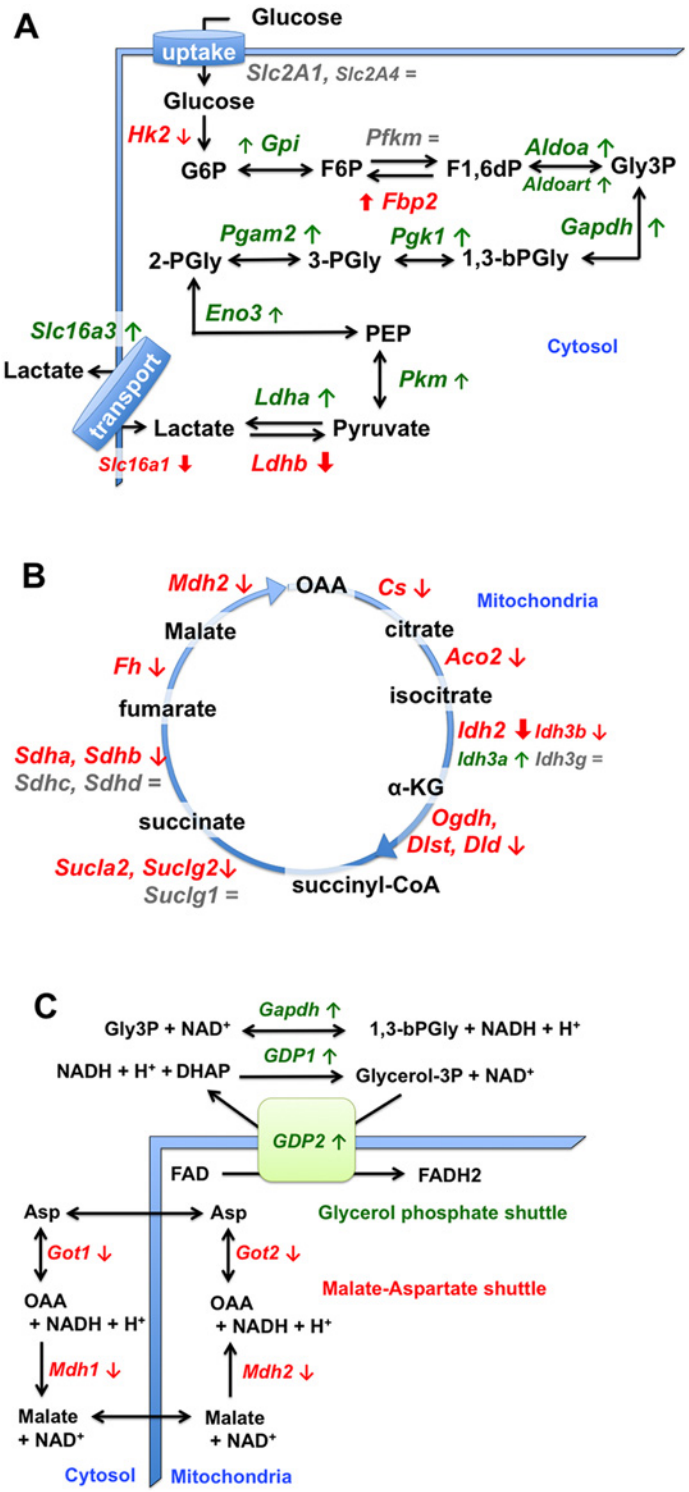

Fig 2. Changes in glycolytic, TCA cycle and mitochondrial shuttle genes in gastrocnemius muscle after olanzapine infusion. Effects of olanzapine infusion on muscle gene expression are shown for the glycolysis pathway (A), citric acid (TCA) cycle (B) and two mitochondrial shuttles (C; the mitochondrial malate, *SLC25A11*, and aspartate, *SLC25A13*, transporters were not affected). The blue lines indicate the sarcolemma (A) or the mitochondrial membrane (C). Metabolites and glycolytic intermediates are shown in black font; gene names are *italicized*. Arrows indicate an increase (↑, ⬆) or decrease (↓, ⬇) in gene expression due to olanzapine infusion; bold arrows indicate a larger magnitude of change. Gray font and

equal sign (=) indicates no significant change. Colored font indicates a change predicted to oppose (red) or promote (green) the pathway. Where the abundance of two isoforms is different, the font size is smaller for the isoform where the FPKM has a lower value (S3 Table).

doi:10.1371/journal.pone.0123966.g002

in skeletal muscle and/or an increase in muscle associated adipose tissue. Further studies would be needed to examine these ideas.

Several genes responsible for mitochondrial BCAA oxidation [65] were decreased by olanzapine (S4 Table), including the catalytic subunit of branched chain keto acid dehydrogenase (*BCKDHA*) and the next step in leucine metabolism catalyzed by isovaleryl-CoA dehydrogenase (*IVD*). Both of these are obesity or diabetes candidate genes [49].

Consistent with the down regulation of genes in glucose, amino acid and fatty acid oxidation, IPA pathway analysis of gene expression indicated that a canonical pathway termed "Mitochondrial Dysfunction" was increased by olanzapine. While many of the genes in this pathway were only modestly affected, those effects were individually highly significant and when taken together as a pathway it was the most significantly affected process with P = 1.9e-46 (S5 Table). These 72 genes largely comprise mitochondrial and nuclear-encoded mitochondrial genes in the oxidative phosphorylation pathway, including complexes I–V.

To summarize, a third piece of evidence supporting a transition to a more glycolytic type (IIb) arises from the observation of a general increase in glycolytic genes and diminution in

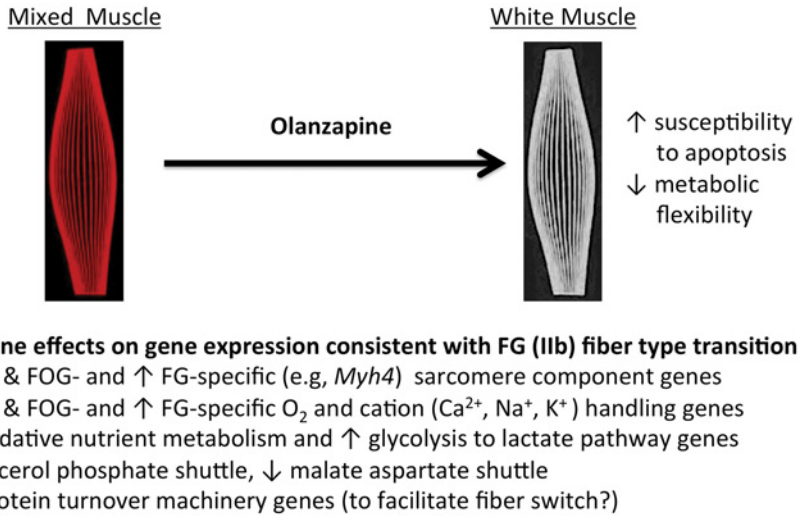

Fig 3. Simplified schematic summarization of muscle fiber types and the pathways affected by olanzapine infusion in skeletal muscle. Striated skeletal muscle fibers can be categorized into three or more different types such as (1) slow-twitch oxidative (SO, red), type I, (2) fast-twitch oxidative-glycolytic (FOG, intermediate twitch) and in rats (3) the fastest-twitch glycolytic (FG, white), type IIb. Gastrocnemius, the muscle examined in this paper, normally contains all of these. Fiber types differ in twitch speed and metabolic flexibility. They are frequently categorized into the above types based one or more of the following: myosin heavy chain isoform content or myosin ATPase activity or gene expression. Compared to SO fibers, FG fibers have: (a) fewer mitochondria, reduced vascularity and myoglobin (*Mb*) for O_2 handling making them whiter in appearance compared to the redder SO fibers; (b) lower expression of genes in FFA, glucose and amino acid oxidation pathways, (c) increased expression of most genes in the glycolysis to lactate pathway; (d) different NADH shuttles; (e) fiber type specific expression of specific sarcomere components, and (f) specific isoforms of calcium and monovalent cation handling or transport proteins. Our data suggest that acute exposure to olanzapine is beginning a process that will eventually cause a fiber type transition from a mixed type to a whiter FG (IIb) type. Whiter muscle has been reported to be more susceptible than other fiber types to atrophy, and such fiber type transitions changes are associated with metabolic disease and obesity.

doi:10.1371/journal.pone.0123966.g003

Table 2. Statistically significant effects of olanzapine on the expression of genes involved in oxidative lipid metabolism.

Gene name	Vehicle, FPKM[1]	Olanzapine, FPKM[1]	Normalized fold change	Molecular identity
Acaa2 *	233±40	145±8	-1.7	Acetyl-CoA acyltransferase 2
Acad9	31±5	14±2	-2.2	Acyl-CoA dehydrogenase family, member 9
Acadl	384±72	221±8	-1.8	Acyl-CoA dehydrogenase, long chain
Acadm	426±47	245±18	-1.8	Acyl-CoA dehydrogenase, C-4 to C-12 straight chain
Acads *	102±13	78±8	-1.4	Acyl-CoA dehydrogenase, C-2 to C-3 short chain
Acadsb	31±7	18±2	-1.8	Acyl-CoA dehydrogenase, short/ branched chain
Acat1	285±45	210±19	-1.4	Acetyl-CoA acetyltransferase, mitochondrial also known as acetoacetyl-CoA thiolase
Acadvl *	163±16	101±5	-1.7	Acyl-CoA dehydrogenase, very long chain
Acox1	24±1	16±2	-1.6	Acyl-CoA oxidase 1, palmitoyl
Acsl1	139±28	73±12	-2.0	Ayl-CoA synthetase long-chain family member 1
Acss1	20±3	4.7±0.7	-4.5	Acetyl-CoA synthetase, mitochondrial
Acss2	19±4	12±0.1	-1.7	Acetyl-coenzyme A synthetase, cytoplasmic
Alox15	9.1±7.0	1.9±0.5	-2.2	Arachidonate 15-lipoxygenase
Cd36	40±8	24±2	-1.7	Fatty acid translocase (transmembrane)
Cpt1b	131±11	91±6	-1.5	Carnitine palmitoyltransferase 1b, muscle
Cpt2	67±11	40±3	-1.7	Carnitine palmitoyltransferase 2
Eci1	142±15	103±10	-1.4	Enoyl-CoA delta isomerase 1
Ech1 *	277±32	236±4	-1.2	Enoyl Coenzyme A hydratase 1, peroxisomal
Fabp3	1386±251	633±68	-2.3	Fatty acid binding protein 3, muscle
Fabp4	277±25	383±90	+1.3	Fatty acid binding protein 4, adipocyte
Hadh	94±13	49±1	-2.0	Medium and short-chain L-3-hydroxyacyl-coenzyme A dehydrogenase, mitochondrial
Hadha	262±25	151±8	-1.8	Trifunctional protein, alpha subunit
Hadhb	447±75	328±3	-1.4	Trifunctional protein, beta subunit
Lpl *	174±31	51±15	-3.5	Lipoprotein Lipase
Slc25a20	84±11	52±2	-1.7	Carnitine/acylcarnitine translocase (cytosol mitochondrial)
Slc27a1 *	11±1	4±1	-2.8	Solute carrier family 27 (Fatty acid transporter), Member 1
UCP3	23±7	44±18	+1.9	Uncoupling protein 3, mitochondrial

The role of these genes in lipid metabolism was determined from RGD, KEGG, Genecards and/or IPA websites as described in Methods. Results are mean ± SE of FPKM gene expression values or normalized fold changes found to be statistically significant using the DEGSeq R package. An asterisk (*) indicates one of 164 prioritized obesity or T2D candidate genes from a previous study [49]. The corresponding molecular identity and database number is in S1 Table.

doi:10.1371/journal.pone.0123966.t002

those for oxidation of glucose, lipid and branched chain amino acids, consistent with the known metabolic differences between muscle fiber types [56, 59, 66].

Olanzapine effects on genes related to protein turnover

In order to transition from one fiber type to another, the sarcomeric and non-sarcomeric components specific to the slower fiber types would have to be degraded and replaced with new components found in IIb fibers. Gene expression and pathway analyses are consistent with this idea. Pathway analysis revealed increases in the EIF2 Signaling pathway for global protein synthesis and genes involved in apoptosis and proteosomal mediated degradation. Specifically, olanzapine up-regulated forty-nine genes ($p = 1.9e-21$) in the EIF-2 signaling-protein synthesis pathway, these include several dozen ribosomal protein genes (Table 3). Ingenuity pathway

Table 3. Canonical EIF2-signaling pathway/ protein synthetic machinery genes statistically altered by olanzapine infusion in gastrocnemius.

Gene name	Vehicle, FPKM[1]	Olanzapine, FPKM[1]	Normalized fold change	Molecular Identity
Akt2	80±1	101±5	1.2	v-akt murine thymoma viral oncogene homolog 2
Eif2s2	50±6	73±6	1.4	eukaryotic translation initiation factor 2, subunit 2 beta, 38kDa
Eif3i	40±4	57±2	1.4	eukaryotic translation initiation factor 3, subunit I
Eif4a2	210±30	246±25	1.13	eukaryotic translation initiation factor 4A2
Fau	45±11	65±17	1.4	Finkel-Biskis-Reilly murine sarcoma virus (FBR-MuSV) ubiquitously expressed (chr1: 228355747–228357261)
Hras1	31±1	64±4	2.0	Harvey rat sarcoma viral oncogene homolog
Ppp1ca	137±15	187±21	1.3	protein phosphatase 1, catalytic subunit, alpha isozyme
Ppp1cb	133±18	119±8.5	-1.2	protein phosphatase 1, catalytic subunit, beta isozyme
Rpl10	185±23	233±30	1.2	ribosomal protein L10
Rpl11	317±28	429±57	1.3	ribosomal protein L11
Rpl12	0.6±0.3	10±4	18.6	ribosomal protein L12 (chr3:17346298–17348585)
Rpl13a	65±6	88±14	1.3	ribosomal protein L13a
Rpl14	190±17	254±25	1.3	ribosomal protein L14
Rpl17	26±12	38±19	1.4	ribosomal protein L17
Rpl18	202±13	262±26	1.3	ribosomal protein L18
Rpl18a	604±56	763±83	1.2	ribosomal protein L18a
Rpl19	190±18	229±19	1.2	ribosomal protein L19
Rpl23	329±14	442±49	1.3	ribosomal protein L23
Rpl24	239±37	327±47	1.3	ribosomal protein L24
Rpl26	29±6	44±11	1.5	ribosomal protein L26
Rpl27	100±13	153±19	1.5	ribosomal protein L27
Rpl28	190±21	275±38	1.4	ribosomal protein L28, (RGD1565183)
Rpl3	62±3	90±14	1.4	ribosomal protein L3
Rpl30	10±9	37±18	3.6	ribosomal protein L30
Rpl35	275±31	360±33	1.3	ribosomal protein L35
Rpl37a	75±20	136±19	1.7	ribosomal protein L37a
Rpl4	254±31	377±44	1.4	ribosomal protein L4
Rpl41	384±24	570±98	1.4	ribosomal protein L41
Rpl7	181±20	227±23	1.2	ribosomal protein L7
Rplp0	747±27	969±93	1.3	ribosomal protein, large, P0
Rplp1	75±20	111±29	1.3	ribosomal protein, large, P1
Rps10l1	37±5	59±8	1.5	ribosomal protein S10 (chr6:84968906–84969452)
Rps11	302±11	395±37	1.3	ribosomal protein S11
Rps13	28±3	41±5	1.4	ribosomal protein S13
Rps15	356±28	516±64	1.4	ribosomal protein S15
Rps15a	15±0.5	22±3	1.5	ribosomal protein S15a
Rps16	254±22	395±57	1.5	ribosomal protein S16
Rps18	53±7	76±11	1.4	ribosomal protein S18
Rps2	20±6	33±5	1.6	ribosomal protein S2
Rps23	74±6	109±12	1.4	ribosomal protein S23
Rps24	101±14	139±22	1.4	ribosomal protein S24
Rps25	19±3	28±3	1.4	ribosomal protein S25
Rps27	380±38	512±86	1.3	ribosomal protein S27
Rps27a	141±9	210±44	1.4	ribosomal protein S27a
Rps27l	90±10	167±23	1.8	ribosomal protein S27-like

(*Continued*)

Table 3. (*Continued*)

Gene name	Vehicle, FPKM[1]	Olanzapine, FPKM[1]	Normalized fold change	Molecular Identity
Rps29	408±38	470±22	1.1	ribosomal protein S29
Rps3	195±11	280±46	1.4	ribosomal protein S3
Rps5	445±28	541±22	1.2	ribosomal protein S5
Rps7	75±8	106±17	1.4	ribosomal protein S7 (chr5:172581803–172582388)
Rps7	35±3	53±8	1.4	ribosomal protein S7(chr6:56601564–56606473)
Rpsa	240±14	351±50	1.4	ribosomal protein SA

Genes from the canonical pathway from Ingenuity Pathway Analysis that were significantly affected by olanzapine treatment are shown.

doi:10.1371/journal.pone.0123966.t003

analysis predicted that apoptosis was also preparing to be activated (Z-score of 2.6) with 142 genes affected (p = 1.4e-16, data not shown). In addition, two of four key genes associated with proteolysis, catabolic disorders and atrophy in skeletal muscle, *TRIM63* (MuRF1) and *Ddit4l* (REDD2) [67, 68], were significantly up regulated (~1.4–1.5 norm FC), whereas two others, Ddit4 (REDD1) and Fbxo32 (atrogin-1) were not affected (S1 Table). Olanzapine also up-regulated the expression of genes involved in the 20S core particle of the proteosome including: *PSMB1*, *PSMB4*, *PSMB5*, *PSMB6*, *PSMB7*, *PSMA7*, along with genes for several ubiquitin-conjugating enzymes: *UBE2E2*, *UBE2G1*, *UBE2G2 and UBE2S* (S1 Table).

Canonical and upstream pathway analysis

In addition to the canonical pathways mentioned earlier (e.g., glycolysis, lipid metabolism, EIF-2 signaling/protein synthesis pathway, apoptosis, etc.), bioinformatics implicated other pathways (S6 and S7 Tables) and predicted upstream pathways affected by olanzapine (S8 Table). Both Integrin Linked kinase (ILK Pathway, 43 genes significantly affected, p = 1.3e-16, S6 Table) and Calcium Sensing pathways (39 genes significantly affected, p = 2.3e-14, S7 Table) were affected by olanzapine. Both have been previously linked to muscle fiber transitions.

In terms of potential mechanisms for these effects, we can first consider one involving elevated glucocorticoids (NCBI Geo profile GDS2688) [32]. Olanzapine elevates glucocorticoids [31], and we did observe a number of glucocorticoid response genes up regulated by olanzapine. For example, metallothioneins such as *Mt1m*, *Mt2A* were significantly up regulated as were *Art3*, *Ankrd9*, *Cebpd*, *Dapk1*, *Eif4ebp1*, *Gadd45g*, *IL15*, *Sar1b*, *Serpina3n*, *Slc30a2*, *Sult1a1*, *Thrsp*, *VPS45* (S1 Table). However other genes that are induced by methylprednisolone in skeletal muscle during time course studies) [32], were either not affected (e.g., *Ddit4*, *Trim63*) or down regulated by olanzapine (e.g., *LPL*, *Csrp3*). Furthermore most of the changes we observed in genes encoding proteins or enzymes of the sarcomere, glycolysis, lipid metabolism, amino acid metabolism and protein turnover could not be ascribed to this mechanism. Nevertheless, upstream pathway analysis did implicate a large set of other potential regulators (S8 Table).

The top 20 potential regulators from IPA analysis included RICTOR (inhibited), *MYCN* (activated), *MYC*, insulin and IGF receptors (inhibited), *TP53*, *PPARGC1A* and *PPARG* (inhibited), *HRAS* (activated) and Huntingtin (*HTT*). For example, inhibition of the rapamycin-insensitive companion of mTOR, *RICTOR* (p = 4.9e-52, Activation Z score: -6.3) was predicted. That pathway includes many of the same genes implicated in ILK and EIF-2α signaling mentioned earlier. Additionally, activation was predicted for the Myc and N-myc proto-oncogene transcription factors, *MYC* (p = 2.3e-51, activation Z score: 2), *MYCN* (p = 1.2E-34, activation Z score: 5.2) along with mitogen-activated protein kinase kinase kinase kinase 4 (*Map4k4*,

p = 8.2e-15, activation Z score: 3.7). However, some growth factor pathways were predicted to be inhibited, including vascular endothelial growth factor A (*VEGF*, whose expression was also significantly decreased, S2 Table, p = 2e-15 for the pathway, Activation Z score: -2.5), transforming growth factor beta 1 (*TGFB1*, p = 2.1e-15, Activation Z score: -4.3) and Insulin-like growth factor 1 (*IGF1*, p = 1.3e-10, Activation Z score: -3.2). The loss of genes associated with VEGF signaling is consistent with the observation that fast fibers are less vascularized as cited earlier. Several predicted regulators (S8 Table) also suggest an overall "endocrine disruption". However, there is no known link between any of the above pathways and receptors that olanzapine is known to inhibit.

A potential mechanism for a red to white or a white to "whiter" switch could be increased Calcineurin-A/NFAT signaling associated with the increase in myozenin-1 expression we observed [55]. Myozenin-1 (*MYOZ1*, also called FatZ1) encodes the calsarcin-2 protein. *MYOZ1* expression is restricted to fast skeletal muscle in contrast to myozenin-2 (*MYOZ2*, *FatZ1*) which encodes calsarcin-1, found in adult cardiac and slow-twitch skeletal muscle [55]. Consistently, rat gastrocnemius, which contains a greater number of white than red fibers, had about 72% of its myozenin FPKM values as MYOZ1. MYOZ1 increased, whereas MYOZ2 decreased after olanzapine treatment (Table 1 and S1 Table). Knock-out mouse studies suggest that myozenins act as a brake on calcineurin signaling which plays a critical role in the promotion of fast-twitch fibers [55]. Myoz1 KO mice have similar muscle size, lower body weight and more slow oxidative muscle fibers [42]. Chronic olanzapine treatment causes greater adiposity without a change in body weight implying a loss of lean mass [17, 18], and in this study a greater expression of Myoz1 in skeletal muscle and other evidence of fiber type changing to the fastest twitch type, IIb. Other findings consistent with a role for Calcineurin-A/NFAT signaling/loss of lean mass are the alterations in ILK, Rictor and Calcium Signaling pathways mentioned earlier along with evidence of deceased Insulin receptor and IGF-1 Receptor Signaling pathways observed (S8 Table). Nevertheless, it is unclear how olanzapine would increase myosenin-1. Albeit, this is also the case for a number of the earlier described upstream pathways found to be affected through Ingenuity Pathway Analysis, with the exception of the activation of the corticosteroid response genes due to the rise in glucocorticoids initiated by olanzapine [31].

Conclusions

In summary, our data indicate that at doses that cause a mild hyperglycemia, much less than that observed acutely with higher doses of the drug [31], olanzapine is eliciting a rapid and dramatic effect on the expression of a host of skeletal muscle genes that appears to be aimed at switching the muscle fiber type along with associated metabolism from a slower (more oxidative) to a faster (more glycolytic) fiber type (Fig 3). Studies have previously shown that olanzapine exerts acute effects leading to increased plasma glucose, impaired hepatic glucose and muscle glucose metabolism while dramatically increasing the use of fat as a fuel [12–14, 18, 31, 69, 70]. It might seem counter intuitive therefore that the response of muscle to that situation would be to switch to a fiber type that was less metabolically flexible and less able to oxidize fat. However in insulin resistant obesity and T2D, there is also an increase of use of fat as a fuel as the muscle becomes unable to transport glucose and in those metabolic states skeletal muscle also undergoes similar fiber type transitions from more oxidative to more glycolytic [24–27]. A muscle fiber type transition could be important in the setting of olanzapine inducing adiposity because such a transition might decrease the basal energy requirements of lean tissue. This in turn could lead to a surfeit of energy that along with other factors promote the adiposity that is observed in humans and animal models treated with olanzapine. In addition to differences in resting energy requirements and fuel selection, fast-twitch glycolytic fibers are also more

susceptible to atrophy arising from various metabolic pathologies compared to slow-twitch oxidative fibers [23]. That could also play a role in the shifts in body composition in observed in animal models and humans treated with SGAs, e.g.: [18]. Finally, these findings are important because a slower to faster muscle fiber type transition may be potentially reversible by the type of exercise that is selected. For example, it is known that endurance exercise training can cause the reverse effect, fast to slow twitch transitions [71].

Supporting Information

S1 Fig. Correlation between RNA-Seq and QT-RTPCR data. Comparison of gene expression changes after olanzapine infusion as measured by QT-RTPCR and RNA-Seq.
(TIFF)

S1 Table. Selected output and FPKM results from Cufflinks analysis and descriptive statistics. This table contains the following Excel column headers: A—ENSEMBLE Gene ID; B—Official Gene Symbol (gene_short); C—Gene locus (locus, chr1 = chromosome 1 etc.); D—Control animal #3 (FKPM units); E—Olanzapine treated animal #4 (FKPM units); F—Control animal #9 (FKPM units); G—Olanzapine treated animal #10 (FKPM units); H—Control animal #11 (FKPM units); I—Olanzapine treated animal #12 (FKPM values); J—Mean—Control group (C-mean, FKPM units); K—Standard Error of the Mean—Control group (C-SE, FKPM units); L—Mean—Olanzapine group units = FKPM (Ola-mean, FKPM units); M—Standard Error of the Mean—Olanzapine group (Ola-SE, FKPM units); N—Normalized fold change from S2 Table 3; O—$p<0.05$? True = 1, False = 0 from S2 Table; P—$p<0.001$? True = 1, False = 0 from S2 Table
(XLSX)

S2 Table. Statistical analysis of RNA Seq data, output from DEGseq 1.18.0 R package. This table contains the following Excel column headers: A—ENSEMBLE Gene ID; B—Sum of Olanzapine FPKM values for all three animals; C—Sum of Control FPKM values; D—$\log_2$ fold change Olanzapine/Control; E—$\log_2$ (fold change) Normalized; F—p-value comparing olanzapine to control; G—q-value (method 1 Benjamini et al. 1995); H—q-value (method 2 Storey et al. 2003); I—Signature (p-value < 0.001); J—Normalized fold change; K—$p<0.05$? True = 1, False = 0; L—$p<0.001$? True = 1, False = 0.
(XLSX)

S3 Table. Glycolytic, TCA Cycle and Mitochondrial Shuttle Gene Expression in Gastrocnemius Muscle after Olanzapine Infusion. Table annotated in the file.
(PDF)

S4 Table. Olanzapine inhibition of Skeletal Muscle Genes in Branched Chain Amino Acid oxidation. Table annotated in the file.
(PDF)

S5 Table. Genes altered by Olanzapine in Canonical Mitochondrial Dysfunction Pathway. Table annotated in the file.
(PDF)

S6 Table. Genes altered by Olanzapine in Canonical ILK Pathway. This table contains the following Excel column headers: A—Symbol; B—Entrez Gene Name; C—Ensembl; D—Fold Change; E—Location; F—Type; G—Biomarker Application(s); H—Drug(s); I—Entrez Gene ID for Human; J—Entrez Gene ID for Mouse; K—Entrez Gene ID for Rat
(XLS)

S7 Table. Genes altered by Olanzapine in Calcium Signaling Pathway. This table contains the following Excel column headers: A—Symbol; B—Entrez Gene Name; C—Ensembl; D—Fold Change; E—Location; F—Type; G—Biomarker Application(s); H—Drug(s); I—Entrez Gene ID for Human; J—Entrez Gene ID for Mouse; K—Entrez Gene ID for Rat
(XLS)

S8 Table. Potential Upstream Regulators. Upstream regulators from Ingenuity Pathway Analysis. The table contains the following Excel column headers: A—Upstream Regulator; B—Fold Change; C—Molecule Type; D—Predicted Activation State; E—Activation z-score; F—p-value of overlap; G—Target molecules in dataset; H—Mechanistic Network
(XLSX)

Acknowledgments

The authors wish to thank Christopher Yengo and Charles Lang for helpful discussions.

Author Contributions

Conceived and designed the experiments: CJL YX AH. Performed the experiments: YX CJL AH YIK. Analyzed the data: CJL YX AH ACS YIK. Contributed reagents/materials/analysis tools: YIK AH CJL. Wrote the paper: CJL AH ACS YIK.

References

1. Maher AR, Theodore G. Summary of the comparative effectiveness review on off-label use of atypical antipsychotics. J Manag Care Pharm. 2012; 18(5 Suppl B):S1–20. PMID: 22784311.
2. Towbin KE. Gaining: pediatric patients and use of atypical antipsychotics. Am J Psychiatry. 2006; 163 (12):2034–6. Epub 2006/12/08. doi: 163/12/2034 [pii] 10.1176/appi.ajp.163.12.2034 PMID: 17151148.
3. Friedman RA. A Call for Caution on Antipsychotic Drugs. The New York Times. 2012: D6.
4. de Leon J, Susce MT, Johnson M, Hardin M, Pointer L, Ruano G, et al. A clinical study of the association of antipsychotics with hyperlipidemia. Schizophr Res. 2007; 92(1–3):95–102. PMID: 17346932.
5. Olfson M, Marcus SC, Corey-Lisle P, Tuomari AV, Hines P, L'Italien GJ. Hyperlipidemia following treatment with antipsychotic medications. Am J Psychiatry. 2006; 163(10):1821–5. PMID: 17012695.
6. eder-Ischia U, Ebenbichler C, Fleischhacker WW. Olanzapine-induced weight gain and disturbances of lipid and glucose metabolism. Essent Psychopharmacol. 2005; 6(2):112–7. PMID: 15765795.
7. Laimer M, Ebenbichler CF, Kranebitter M, Eder U, Mangweth B, Weiss E, et al. Olanzapine-induced hyperglycemia: role of humoral insulin resistance-inducing factors. J Clin Psychopharmacol. 2005; 25(2):183–5. PMID: 15738752.
8. Kyriazis IA, Korovesis K, Bashir S, Liakouras A, Partheniou C. Diabetic ketoacidosis and severe dyslipidemia in an adult psychotic man with olanzapine treatment. J Clin Psychopharmacol. 2006; 26(1):92–4. PMID: 16415716.
9. Hasnain M, Vieweg WV, Hollett B. Weight gain and glucose dysregulation with second-generation antipsychotics and antidepressants: a review for primary care physicians. Postgrad Med. 2012; 124(4):154–67. doi: 10.3810/pgm.2012.07.2577 PMID: 22913904.
10. Deng C. Effects of antipsychotic medications on appetite, weight, and insulin resistance. Endocrinol Metab Clin North Am. 2013; 42(3):545–63. doi: 10.1016/j.ecl.2013.05.006 PMID: 24011886.
11. Newcomer JW. Metabolic considerations in the use of antipsychotic medications: a review of recent evidence. J Clin Psychiatry. 2007; 68 Suppl 1:20–7. PMID: 17286524.
12. Albaugh VL, Vary TC, Ilkayeva O, Wenner BR, Maresca KP, Joyal JL, et al. Atypical antipsychotics rapidly and inappropriately switch peripheral fuel utilization to lipids, impairing metabolic flexibility in rodents. Schizophr Bull. 2012; 38(1):153–66. doi: 10.1093/schbul/sbq053 PMID: 20494946; PubMed Central PMCID: PMC3245588.
13. Hahn MK, Wolever TM, Arenovich T, Teo C, Giacca A, Powell V, et al. Acute effects of single-dose olanzapine on metabolic, endocrine, and inflammatory markers in healthy controls. J Clin Psychopharmacol. 2013; 33(6):740–6. doi: 10.1097/JCP.0b013e31829e8333 PMID: 24100786.

14. Albaugh VL, Singareddy R, Mauger D, Lynch CJ. A double blind, placebo-controlled, randomized crossover study of the acute metabolic effects of olanzapine in healthy volunteers. PLoS One. 2011; 6 (8):e22662. doi: 10.1371/journal.pone.0022662 PMID: 21857944; PubMed Central PMCID: PMC3153475.

15. Vidarsdottir S, de Leeuw van Weenen JE, Frolich M, Roelfsema F, Romijn JA, Pijl H. Effects of Olanzapine and Haloperidol on the Metabolic Status of Healthy Men. J Clin Endocrinol Metab. 2009. Epub 2009/11/13. doi: jc.2008-1815 [pii] 10.1210/jc.2008-1815 PMID: 19906788.

16. Kaddurah-Daouk R, McEvoy J, Baillie RA, Lee D, Yao JK, Doraiswamy PM, et al. Metabolomic mapping of atypical antipsychotic effects in schizophrenia. Mol Psychiatry. 2007; 12(10):934–45. Epub 2007/04/19. doi: 4002000 [pii] 10.1038/sj.mp.4002000 PMID: 17440431.

17. Albaugh VL, Henry CR, Bello NT, Hajnal A, Lynch SL, Halle B, et al. Hormonal and metabolic effects of olanzapine and clozapine related to body weight in rodents. Obesity (Silver Spring). 2006; 14(1):36–51. Epub 2006/02/24. doi: 10.1038/oby.2006.6 PMID: 16493121; PubMed Central PMCID: PMC2761763.

18. Albaugh VL, Judson JG, She P, Lang CH, Maresca KP, Joyal JL, et al. Olanzapine promotes fat accumulation in male rats by decreasing physical activity, repartitioning energy and increasing adipose tissue lipogenesis while impairing lipolysis. Mol Psychiatry. 2011; 16(5):569–81. doi: 10.1038/mp.2010.33 PMID: 20308992; PubMed Central PMCID: PMC2892549.

19. Ader M, Kim SP, Catalano KJ, Ionut V, Hucking K, Richey JM, et al. Metabolic dysregulation with atypical antipsychotics occurs in the absence of underlying disease: a placebo-controlled study of olanzapine and risperidone in dogs. Diabetes. 2005; 54(3):862–71. PMID: 15734866.

20. MacIntosh BR, Gardiner PF, McComas AJ, McComas AJ. Skeletal muscle: form and function. Champaign, IL: Human Kinetics; 2006. viii, 423 p. p.

21. Schiaffino S, Reggiani C. Fiber types in mammalian skeletal muscles. Physiol Rev. 2011; 91(4):1447–531. doi: 10.1152/physrev.00031.2010 PMID: 22013216; PubMed Central PMCID: PMC22013216.

22. Smerdu V, Karsch-Mizrachi I, Campione M, Leinwand L, Schiaffino S. Type IIx myosin heavy chain transcripts are expressed in type IIb fibers of human skeletal muscle. Am J Physiol. 1994; 267(6 Pt 1): C1723–8. PMID: 7545970; PubMed Central PMCID: PMC7545970.

23. Wang Y, Pessin JE. Mechanisms for fiber-type specificity of skeletal muscle atrophy. Curr Opin Clin Nutr Metab Care. 2013; 16(3):243–50. doi: 10.1097/MCO.0b013e328360272d PMID: 23493017; PubMed Central PMCID: PMC4327989.

24. He J, Watkins S, Kelley DE. Skeletal muscle lipid content and oxidative enzyme activity in relation to muscle fiber type in type 2 diabetes and obesity. Diabetes. 2001; 50(4):817–23. PMID: 11289047; PubMed Central PMCID: PMC11289047.

25. Nagatomo F, Fujino H, Kondo H, Gu N, Takeda I, Ishioka N, et al. PGC-1alpha mRNA level and oxidative capacity of the plantaris muscle in rats with metabolic syndrome, hypertension, and type 2 diabetes. Acta Histochem Cytochem. 2011; 44(2):73–80. doi: 10.1267/ahc.10041 PMID: 21614168; PubMed Central PMCID: PMC3096084.

26. Fujita N, Nagatomo F, Murakami S, Kondo H, Ishihara A, Fujino H. Effects of hyperbaric oxygen on metabolic capacity of the skeletal muscle in type 2 diabetic rats with obesity. ScientificWorldJournal. 2012; 2012:637978. doi: 10.1100/2012/637978 PMID: 22778702; PubMed Central PMCID: PMC3385605.

27. Oberbach A, Bossenz Y, Lehmann S, Niebauer J, Adams V, Paschke R, et al. Altered fiber distribution and fiber-specific glycolytic and oxidative enzyme activity in skeletal muscle of patients with type 2 diabetes. Diabetes Care. 2006; 29(4):895–900. PMID: 16567834; PubMed Central PMCID: PMC16567834.

28. Mogensen M, Sahlin K, Fernstrom M, Glintborg D, Vind BF, Beck-Nielsen H, et al. Mitochondrial respiration is decreased in skeletal muscle of patients with type 2 diabetes. Diabetes. 2007; 56(6):1592–9. doi: 10.2337/db06-0981 PMID: 17351150; PubMed Central PMCID: PMC17351150.

29. Ritov VB, Menshikova EV, He J, Ferrell RE, Goodpaster BH, Kelley DE. Deficiency of subsarcolemmal mitochondria in obesity and type 2 diabetes. Diabetes. 2005; 54(1):8–14. PMID: 15616005; PubMed Central PMCID: PMC15616005.

30. Fertuzinhos S, Li M, Kawasawa YI, Ivic V, Franjic D, Singh D, et al. Laminar and temporal expression dynamics of coding and noncoding RNAs in the mouse neocortex. Cell Rep. 2014; 6(5):938–50. doi: 10.1016/j.celrep.2014.01.036 PMID: 24561256; PubMed Central PMCID: PMC3999901.

31. Assie MB, Carilla-Durand E, Bardin L, Maraval M, Aliaga M, Malfetes N, et al. The antipsychotics clozapine and olanzapine increase plasma glucose and corticosterone levels in rats: comparison with aripiprazole, ziprasidone, bifeprunox and F15063. Eur J Pharmacol. 2008; 592(1–3):160–6. Epub 2008/07/22. doi: S0014-2999(08)00718-8 [pii] 10.1016/j.ejphar.2008.06.105 PMID: 18640111.

32. Almon RR, DuBois DC, Yao Z, Hoffman EP, Ghimbovschi S, Jusko WJ. Microarray analysis of the temporal response of skeletal muscle to methylprednisolone: comparative analysis of two dosing regimens. Physiol Genomics. 2007; 30(3):282–99. doi: 10.1152/physiolgenomics.00242.2006 PMID: 17473217.

33. Wang Z, Gerstein M, Snyder M. RNA-Seq: a revolutionary tool for transcriptomics. Nat Rev Genet. 2009; 10(1):57–63. doi: 10.1038/nrg2484 PMID: 19015660; PubMed Central PMCID: PMC19015660.

34. Chauvigne F, Cauty C, Ralliere C, Rescan PY. Muscle fiber differentiation in fish embryos as shown by in situ hybridization of a large repertoire of muscle-specific transcripts. Dev Dyn. 2005; 233(2):659–66. doi: 10.1002/dvdy.20371 PMID: 15844199; PubMed Central PMCID: PMC15844199.

35. McGrath MJ, Cottle DL, Nguyen MA, Dyson JM, Coghill ID, Robinson PA, et al. Four and a half LIM protein 1 binds myosin-binding protein C and regulates myosin filament formation and sarcomere assembly. J Biol Chem. 2006; 281(11):7666–83. doi: 10.1074/jbc.M512552200 PMID: 16407297.

36. Tiso N, Rampoldi L, Pallavicini A, Zimbello R, Pandolfo D, Valle G, et al. Fine mapping of five human skeletal muscle genes: alpha-tropomyosin, beta-tropomyosin, troponin-I slow-twitch, troponin-I fast-twitch, and troponin-C fast. Biochem Biophys Res Commun. 1997; 230(2):347–50. doi: 10.1006/bbrc.1996.5958 PMID: 9016781.

37. Burniston JG, Meek TH, Pandey SN, Broitman-Maduro G, Maduro MF, Bronikowski AM, et al. Gene expression profiling of gastrocnemius of "minimuscle" mice. Physiol Genomics. 2013; 45(6):228–36. doi: 10.1152/physiolgenomics.00149.2012 PMID: 23362141; PubMed Central PMCID: PMC3615581.

38. Carroll SL, Klein MG, Schneider MF. Decay of calcium transients after electrical stimulation in rat fast- and slow-twitch skeletal muscle fibres. J Physiol. 1997; 501 (Pt 3):573–88. PMID: 9218218; PubMed Central PMCID: PMC1159459.

39. Mullen AJ, Barton PJ. Structural characterization of the human fast skeletal muscle troponin I gene (TNNI2). Gene. 2000; 242(1–2):313–20. PMID: 10721725; PubMed Central PMCID: PMC10721725.

40. Thompson CB, McDonough AA. Skeletal muscle Na,K-ATPase alpha and beta subunit protein levels respond to hypokalemic challenge with isoform and muscle type specificity. J Biol Chem. 1996; 271(51):32653–8. PMID: 8955095; PubMed Central PMCID: PMC8955095.

41. Kim JW, Kwon OY, Kim MH. Differentially expressed genes and morphological changes during lengthened immobilization in rat soleus muscle. Differentiation. 2007; 75(2):147–57. doi: 10.1111/j.1432-0436.2006.00118.x PMID: 17316384.

42. Frey N, Frank D, Lippl S, Kuhn C, Kogler H, Barrientos T, et al. Calsarcin-2 deficiency increases exercise capacity in mice through calcineurin/NFAT activation. J Clin Invest. 2008; 118(11):3598–608. doi: 10.1172/JCI36277 PMID: 18846255; PubMed Central PMCID: PMC2564612.

43. Agarkova I, Schoenauer R, Ehler E, Carlsson L, Carlsson E, Thornell LE, et al. The molecular composition of the sarcomeric M-band correlates with muscle fiber type. Eur J Cell Biol. 2004; 83(5):193–204. doi: 10.1078/0171-9335-00383 PMID: 15346809.

44. MacArthur DG, North KN. A gene for speed? The evolution and function of alpha-actinin-3. Bioessays. 2004; 26(7):786–95. doi: 10.1002/bies.20061 PMID: 15221860; PubMed Central PMCID: PMC15221860.

45. Zhang Y, Fujii J, Phillips MS, Chen HS, Karpati G, Yee WC, et al. Characterization of cDNA and genomic DNA encoding SERCA1, the Ca(2+)-ATPase of human fast-twitch skeletal muscle sarcoplasmic reticulum, and its elimination as a candidate gene for Brody disease. Genomics. 1995; 30(3):415–24. doi: 10.1006/geno.1995.1259 PMID: 8825625.

46. Yano K, Zarain-Herzberg A. Sarcoplasmic reticulum calsequestrins: structural and functional properties. Mol Cell Biochem. 1994; 135(1):61–70. PMID: 7816057.

47. Cottle DL, McGrath MJ, Cowling BS, Coghill ID, Brown S, Mitchell CA. FHL3 binds MyoD and negatively regulates myotube formation. J Cell Sci. 2007; 120(Pt 8):1423–35. doi: 10.1242/jcs.004739 PMID: 17389685.

48. Heizmann CW, Berchtold MW, Rowlerson AM. Correlation of parvalbumin concentration with relaxation speed in mammalian muscles. Proc Natl Acad Sci U S A. 1982; 79(23):7243–7. PMID: 6961404; PubMed Central PMCID: PMC347315.

49. Tiffin N, Adie E, Turner F, Brunner HG, van Driel MA, Oti M, et al. Computational disease gene identification: a concert of methods prioritizes type 2 diabetes and obesity candidate genes. Nucleic Acids Res. 2006; 34(10):3067–81. doi: 10.1093/nar/gkl381 PMID: 16757574; PubMed Central PMCID: PMC1475747.

50. Talmadge RJ, Paalani M. Sarco(endo)plasmic reticulum calcium pump isoforms in paralyzed rat slow muscle. Biochim Biophys Acta. 2007; 1770(8):1187–93. doi: 10.1016/j.bbagen.2007.03.013 PMID: 17482761.

51. Wu KD, Lytton J. Molecular cloning and quantification of sarcoplasmic reticulum Ca(2+)-ATPase isoforms in rat muscles. Am J Physiol. 1993; 264(2 Pt 1):C333–41. PMID: 8447366.

52. Yang N, Garton F, North K. alpha-actinin-3 and performance. Med Sport Sci. 2009; 54:88–101. doi: 10.1159/000235698 PMID: 19696509.

53. Norman B, Esbjornsson M, Rundqvist H, Osterlund T, von Walden F, Tesch PA. Strength, power, fiber types, and mRNA expression in trained men and women with different ACTN3 R577X genotypes. J Appl Physiol (1985). 2009; 106(3):959–65. doi: 10.1152/japplphysiol.91435.2008 PMID: 19150855.

54. Ackermann MA, Hu LY, Bowman AL, Bloch RJ, Kontrogianni-Konstantopoulos A. Obscurin interacts with a novel isoform of MyBP-C slow at the periphery of the sarcomeric M-band and regulates thick filament assembly. Mol Biol Cell. 2009; 20(12):2963–78. doi: 10.1091/mbc.E08-12-1251 PMID: 19403693; PubMed Central PMCID: PMC2695803.

55. Laing NG. The sarcomere and skeletal muscle disease. New York, N.Y., Austin, Tex.: Springer Science+Business Media; Landes Bioscience; 2008. xxii, 227 p. p.

56. Stevens L, Firinga C, Gohlsch B, Bastide B, Mounier Y, Pette D. Effects of unweighting and clenbuterol on myosin light and heavy chains in fast and slow muscles of rat. Am J Physiol Cell Physiol. 2000; 279(5):C1558–63. PMID: 11029303.

57. Bamford JA, Lopaschuk GD, MacLean IM, Reinhart ML, Dixon WT, Putman CT. Effects of chronic AICAR administration on the metabolic and contractile phenotypes of rat slow- and fast-twitch skeletal muscles. Can J Physiol Pharmacol. 2003; 81(11):1072–82. doi: 10.1139/y03-110 PMID: 14719043.

58. Chen LN, Lyu J, Yang XF, Ji WJ, Yuan BX, Chen MX, et al. Liraglutide ameliorates glycometabolism and insulin resistance through the upregulation of GLUT4 in diabetic KKAy mice. Int J Mol Med. 2013; 32(4):892–900. doi: 10.3892/ijmm.2013.1453 PMID: 23877319.

59. Beha A, Juretschke HP, Kuhlmann J, Neumann-Haefelin C, Belz U, Gerl M, et al. Muscle type-specific fatty acid metabolism in insulin resistance: an integrated in vivo study in Zucker diabetic fatty rats. Am J Physiol Endocrinol Metab. 2006; 290(5):E989–97. doi: 10.1152/ajpendo.00459.2005 PMID: 16380389.

60. Summermatter S, Santos G, Perez-Schindler J, Handschin C. Skeletal muscle PGC-1alpha controls whole-body lactate homeostasis through estrogen-related receptor alpha-dependent activation of LDH B and repression of LDH A. Proc Natl Acad Sci U S A. 2013; 110(21):8738–43. doi: 10.1073/pnas.1212976110 PMID: 23650363; PubMed Central PMCID: PMC3666691.

61. Simoneau JA, Kelley DE. Altered glycolytic and oxidative capacities of skeletal muscle contribute to insulin resistance in NIDDM. J Appl Physiol (1985). 1997; 83(1):166–71. PMID: 9216960.

62. Schantz PG, Sjoberg B, Svedenhag J. Malate-aspartate and alpha-glycerophosphate shuttle enzyme levels in human skeletal muscle: methodological considerations and effect of endurance training. Acta Physiol Scand. 1986; 128(3):397–407. doi: 10.1111/j.1748-1716.1986.tb07993.x PMID: 3491492; PubMed Central PMCID: PMC3491492.

63. Arikawa E, Ma RC, Isshiki K, Luptak I, He Z, Yasuda Y, et al. Effects of insulin replacements, inhibitors of angiotensin, and PKCbeta's actions to normalize cardiac gene expression and fuel metabolism in diabetic rats. Diabetes. 2007; 56(5):1410–20. doi: 10.2337/db06-0655 PMID: 17363743.

64. Wang Z, Kontani Y, Sato Y, Mizuno T, Mori N, Yamashita H. Muscle type difference in the regulation of UCP3 under cold conditions. Biochemical and Biophysical Research Communications. 2003; 305(2):244–9. doi: 10.1016/S0006-291X(03)00730-7 PMID: 12745065

65. Lynch CJ, Adams SH. Branched-chain amino acids in metabolic signalling and insulin resistance. Nat Rev Endocrinol. 2014; 10(12):723–36. doi: 10.1038/nrendo.2014.171 PMID: 25287287.

66. Chemello F, Bean C, Cancellara P, Laveder P, Reggiani C, Lanfranchi G. Microgenomic analysis in skeletal muscle: expression signatures of individual fast and slow myofibers. PLoS One. 2011; 6(2): e16807. doi: 10.1371/journal.pone.0016807 PMID: 21364935; PubMed Central PMCID: PMC3043066.

67. Kelleher AR, Gordon BS, Kimball SR, Jefferson LS. Changes in REDD1, REDD2, and atrogene mRNA expression are prevented in skeletal muscle fixed in a stretched position during hindlimb immobilization. Physiol Rep. 2014; 2(2):e00246. doi: 10.1002/phy2.246 PMID: 24744910; PubMed Central PMCID: PMC3966240.

68. Vary TC, Frost RA, Lang CH. Acute alcohol intoxication increases atrogin-1 and MuRF1 mRNA without increasing proteolysis in skeletal muscle. Am J Physiol Regul Integr Comp Physiol. 2008; 294(6): R1777–89. doi: 10.1152/ajpregu.00056.2008 PMID: 18401005; PubMed Central PMCID: PMC3585419.

69. Klingerman CM, Stipanovic ME, Bader M, Lynch CJ. Second-generation antipsychotics cause a rapid switch to fat oxidation that is required for survival in C57BL/6J mice. Schizophr Bull. 2014; 40(2):327–40. doi: 10.1093/schbul/sbs196 PMID: 23328157; PubMed Central PMCID: PMC3932077.

70. Chintoh AF, Mann SW, Lam L, Lam C, Cohn TA, Fletcher PJ, et al. Insulin resistance and decreased glucose-stimulated insulin secretion after acute olanzapine administration. J Clin Psychopharmacol. 2008; 28(5):494–9. Epub 2008/09/17. doi: 10.1097/JCP.0b013e318184b4c5 00004714-200810000-00004 [pii]. PMID: 18794643.

71. Tajsharghi H, Sunnerhagen KS, Darin N, Kyllerman M, Oldfors A. Induced shift in myosin heavy chain expression in myosin myopathy by endurance training. J Neurol. 2004; 251(2):179–83. doi: 10.1007/s00415-004-0295-5 PMID: 14991352.